Effects of Natural Ageing Treatment on Mechanical, Microstructural and Forming Properties of Al 2024 Aluminum Alloy Sheets

M. Fallah Tafti, M. Sedighi and R. Hashemi*

* *rhashemi@iust.ac.ir*

Received: January 2018 Accepted: August 2018

School of Mechanical Engineering, Iran University of Science and Technology, Tehran, Iran

DOI: 10.22068/ijmse.15.4.1

Abstract: *In this study, the microstructural variations, mechanical properties and forming limit diagrams (FLD) of Al 2024 aluminum alloy sheet with the thickness of 0.81mm are investigated during natural ageing (T4) treatment. The most formability in Al 2024 can be achieved just after solution treatment, and it is better to perform the forming process, on this aluminum alloy sheet, in this condition. However, in industrial applications, there is usually a postponement for some hours after solution treatment to begin the forming process that it means the forming process should be done at the natural ageing condition. This condition decreases the formability of Al 2024 sheets. To monitor the properties variations in natural ageing condition, FLDs were determined after specific times (e.g., 0.5, 1.5, 4 and 24 hours). The variations in micro-hardness, yield strength, ultimate tensile strength and elongation at break were observed with changing the ageing time. The scanning electron microscope (SEM) investigations illustrated that density and size of precipitates were changed with ageing time. Moreover, the Nakazima test was utilized to study the forming limits considering the natural ageing condition. Results showed by increasing the ageing time, up to 4h, the majority of properties variations could be seen, and from 4h to 24h, the variations were changed slower.*

Keywords: *Aluminum alloys, Natural ageing, Solution, Forming limit diagrams.*

1. INTRODUCTION

Aluminum alloys properties can be enhanced by controlling solution and ageing treatment parameters. With ageing at room temperature (natural ageing), the mechanical properties could be stable after some days, especially for 2000 series. Al2024 is one of the practical alloys of aluminum alloys that are used most in the aerospace industry because of its high strength to weight ratio and good fatigue resistance [1]. The mechanical strength and formability are two important factors in sheet metal industries. The ageing heat treatment can improve the mechanical properties of the processed specimen, but it causes decreased on formability properties. So it is essential to investigate the mechanical and formability properties of Al 2024 aluminum alloy sheet during ageing heat treatment.

The strain-based forming limit curve (FLC) that is shown with critical major and minor principal strains is a valuable tool for specifying sheet metal formability [2,3]. Nakazima test is usually used to obtain FLC of sheet metals experimentally [4] according to the ASTM E 2218-02 [5] and the ISO 12004-2 standards [6].

Bagaryatsky [7] studied the phase evolution in Al–Cu–Mg alloys and he introduced four-stage precipitation for ageing, as below:

SSS → GPB zone → S”/GPB2 → S’ → S

By passing of time, the phase supersaturated solid solution (SSS), and GPB transformed into the metastable Al2CuMg (S’), or Al2Cu (θ’) precipitates that they are kind of preform to the S and θ equilibrium particles [8-14]. Different works were performed to examine the role of these precipitates and phases on mechanical properties of the aged Al–Cu–Mg alloys [15–17].

Dilmec et al. [18] investigated the effect of anisotropy and sheet thickness on the formability of AA2024 in T4 condition, experimentally. They used a new method (the interpolation method) for measuring strains by using a grid analysis method. Also, for studying the forming limit curves with more accuracy, they added some new specimens to the regular test specimens, at the plane strain mode, that it improved the accuracy of the FLCs at the plain strain mode. Moy et al. [19] investigated the effect of heat treatment on texture, microstructure, and formability of AA2024 sheets. They aged the sheets with two different thicknesses for different times at a constant temperature 150°C. They performed the ageing at three times- for 2.5hr, two days and one week.

After formability analysis, it concluded that at 2days condition, the formability in plain strain mode was better than other conditions. Afzal et al. [20] studied the mechanical properties and microstructural features of alloy AA2024 in artificially condition. They studied the hardness, tensile test, XRD and microstructural pictures and fractographs analysis at an aged temperature between 105 to 195°C for different times. For the microscopic study, they employed scanning electron microscopy (SEM) and X-ray diffraction (XRD). They illustrated that by variation of the ageing time or temperature, the yield strength, ultimate tensile strength, hardness, plastic elongation and the elastic modulus were changed anomalously. Dilmec et al. [21] investigated the effect of solution heat treatment parameters on formability index and mechanical properties of the AA2024 sheet. They studied the effect of solution temperature, soaking time, heating rate and quenching delay to find the optimal solution heat treatment parameters. They concluded that the best temperature for solution treatment was 493°C and the mechanical properties were decreased with lower and higher temperature. The effect of solution temperature was more than the effect of the quenching delay and soak time. By increasing the quenching delay, the mechanical properties and formability were decreased. Also, the heating rate had a slight effect on these properties.

In this paper, forming limit diagram, mechanical properties and microstructure variations of Al-Cu-Mg alloy sheets at room temperature after solution and during ageing at different times- 0.5, 1.5, 4 and 24 hours are investigated. This is a new result, and this paper adds it to the existing literature that refers mostly to hardness and the evolution of the microstructure during ageing.

2. MATERIALS AND EXPERIMENTAL PROCEDURE

2.1. Material

In the present study, an Al–Cu–Mg alloy sheet with gauge thickness of 0.81mm were utilized. The material chemical composition (in wt. %) was specified by quantometery analysis and is reported in Table 1.

2.2. Heat Treatment Process

The sheets were solution treated at 493°C for 30 minutes [22] and after cold water quenching, age-hardened at room temperature up to 24 hours.

The hardness was measured after solution and different ageing times at 0.5, 1.5, 4 and 24 hours by using a Jenus Vickers Micro-Hardness Testing machines with impressure 200 g load and dwell time 10 second. Uniaxial tensile tests were performed by SANTAM 5KN testing machine. The scanning electron microscopy was applied to study the precipitation variations.

2.3. Experimental Setup For Sheet Metal Forming Limits Determination

The Nakazima test was used to attain FLDs. Fig. 2 displays a schematic view of Nakazima setup; the sides of dies are in according with ISO 12004 standard. The circular grids with 2.5 mm diameter were marked on the surface of the sheet specimens, by using the electrochemical method. For stretching sheet samples, a 5-ton SANTAM STM-50 machine with constant spindle speed was employed. A downfall in the load-displacement diagram was used as the stopping criterion in the test. The specimens with different geometries were utilized to achieve the forming limit curve in this job. Fig. 3 illustrates the geometries of the specimens were used to get FLD [23]. The deformed specimen can be seen in Fig. 4. The experimental FLD setup can be seen in Fig. 5. The circular grids were converted to elliptic shapes after tests. After conducting the Nakazima test for each sample, the limited strains were attained from the major and minor diameters of the ellipse that were located in the closest distance from the necking zone. The major and minor engineering strains were extracted via Equations (2) and (3), and then they were converted into the true strain:

$$\varepsilon_{major}(\%) = \frac{a-c}{c} * 100 \quad (2)$$

$$\varepsilon_{minor}(\%) = \frac{b-c}{c} * 100 \quad (3)$$

Table. 1. Chemical composition (in wt. %) of Al 2024 Alloy

Al	Cu	Mg	Mn	Fe	Si	Cr	Zn	V	Ti	Other
Balance	4.39	0.997	0.453	0.206	0.0904	0.0084	0.0359	0.0134	0.0197	0.098

Where a, b, and c illustrated the ellipse's major and minor diameters and the initial circle diameter, respectively [24].

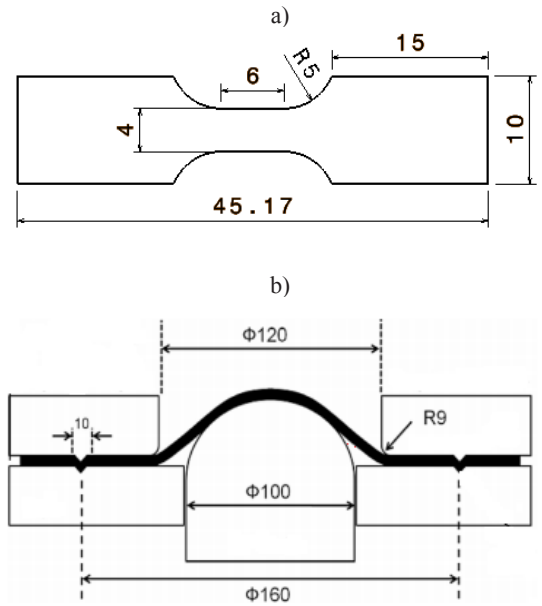

Fig. 2. a) Geometry of tensile test specimen b)Schematic view of the experimental setup for FLDs determination

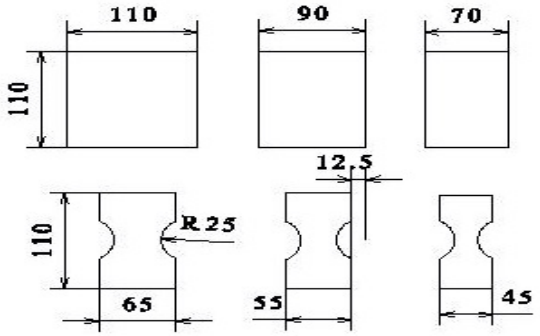

Fig. 3. The specimen geometries were used to determine the FLC[1] (all the dimensions are in mm) [24]

Fig. 4. Typical deformed specimens

1. Forming limit curve

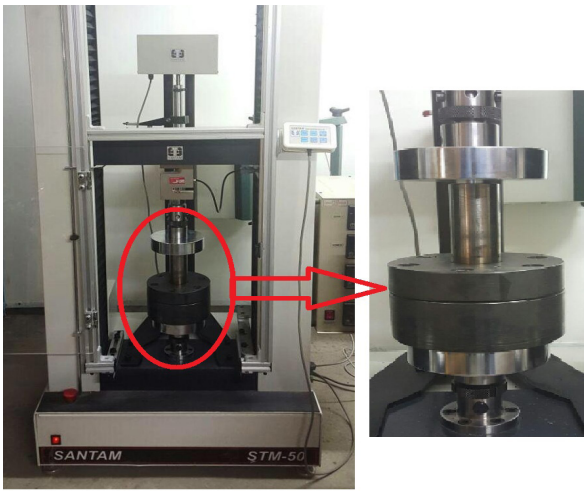

Fig. 5. The experimental FLD equipment

3. RESULTS AND DISCUSSION

3. 1. Tensile Behavior

The mechanical and material properties were achieved by standard tests, using specimens by sub-size geometry. The tests were performed according to ASTM-E08/09 standard, at a constant speed of 3 mm/min. Fig. 6 shows the stress-strain diagrams which were achieved by the uniaxial tensile tests for a solution and aged samples. It can be illustrated that by increasing the ageing time, the yield and the ultimate strength were increased, whereas the elongation to failure was decreased. Based on the different ageing times, changes in the yield strength, the ultimate strength, and the elongation at break, are illustrated in Fig. 7. As be seen by ageing from solution treatment up to 24 hours, the ultimate tensile strength was increased from 313MPa to 411MPa that shows 31% growth and the elongation at break was decreased from 15.4% to 12.9%, which shows 19% reduction.

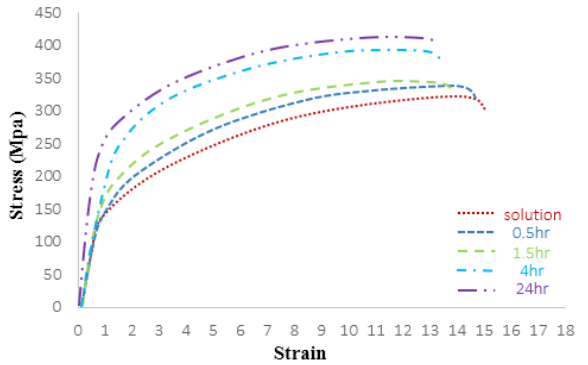

Fig. 6. The true stress-strain curve for heat treated samples

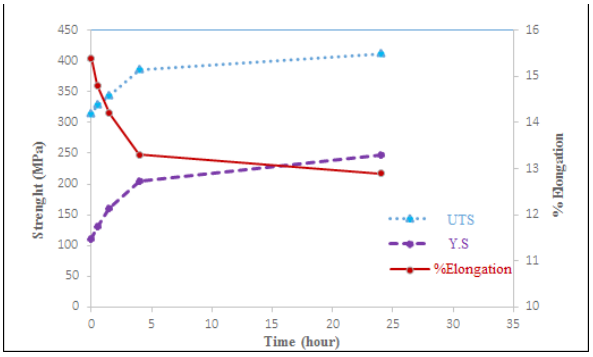

Fig. 7. Changes in the ultimate strength, yield strength, and elongation at break based on the heat treated samples

3. 2. Micro-Hardness Investigation

The hardness contribution is related to some reasons, such as the distribution and size of particles or precipitations, coherency of this precipitation to the alloy matrix and abutment of the particles. The cause of hardness growth is related to changing the stress field environs the precipitates. After solution treatment and quenching, some clusters could be formed, and they caused local strain that results in hardness increasing. By continued ageing, by producing of larger aggregations of Cu atoms on a specific plane of the alloy matrix (θ''), the hardness increased more. Then, some of the precipitate platelets of θ' that has a coherency with the matrix, created and could produce a growth strain field and further hardness increasing. Finally, after continuing ageing the equilibrium phase that is incoherent with the alloy matrix, is produced and it is the onset of hardness decreasing [17].

The micro-hardness variation was measured in heat-treated samples are demonstrated in Fig. 8. It is evident that in this alloy by ageing up to 4hr, the hardness, increased to 94% in comparison with the solution treatment. By ageing process from 4hr to 24hr, the variation was with mild slope and the hardness growth just 6.6% in comparison with ageing for 4hr.

According to Fig. 7 the elongation follows an opposite relation to the ultimate and yield strength. These results showed two different viewpoints to the industrialists. The first approach recommends shaping the material in the beginning before ageing process. The second approach recommends to age the sheet first and then form it. This decision usually is made according to the application. For example, if the application needs high strengthening in some position of the sheet that means the sheet needs to be aged initially until getting high resistance to thinning and then shaped, though, the desired shape cannot be achieved [25].

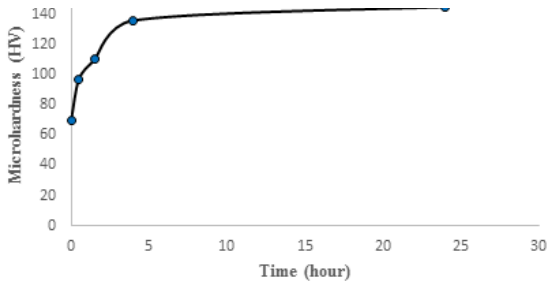

Fig. 8. Changes in micro-hardness based on changing the ageing temperature

3. 3. Forming Limit Diagrams Investigation

After calculating all true limit strains, the FLDs were drawn for five considered temperatures. Fig. 9 illustrates the forming limit diagram after solution treatment. The best formability for this alloy was achieved in this case. The FLD_o for this state is about 0.149. Fig. 10 is demonstrating the FLD for ageing at the time 0.5hr. The FLD_o for this case is about 0.139 that shows 7.2% dropping compared to solution treatment. Fig. 11 show the FLD after 1.5hr. The FLD_o for this condition is about 0.13 that decrease 6.9% compared to previous state (0.5hr). In Fig. 12 could be seen FLD after 4hr. The FLD_o for this condition is about 0.108 that decrease 20% compared to the previous state that it caused experiencing a significant decrease in FLD_o amount, which the cause is: more precipitates distribution. Fig. 13 display the FLD after 24hr. The FLD_o for this condition is about 0.1 that decreased 8% compared to the previous state.

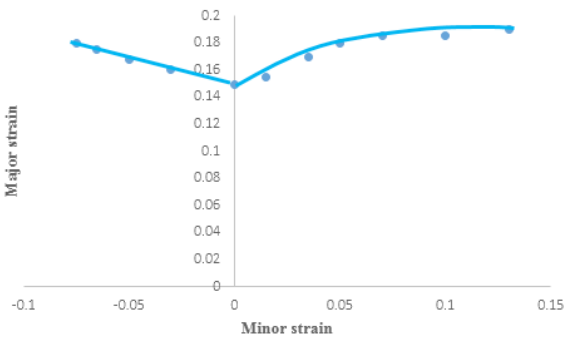

Fig. 9. Forming limit diagram after solution treatment

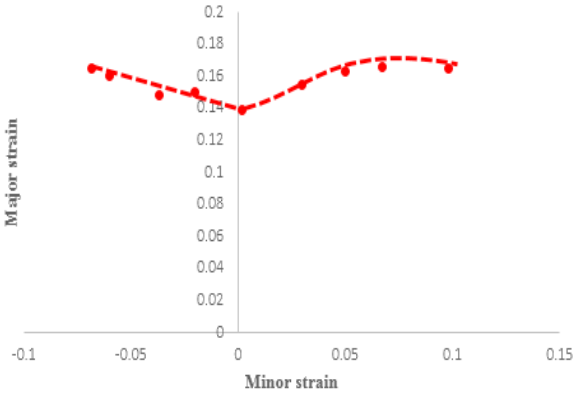

Fig. 10. Forming limit diagram after 0.5hr

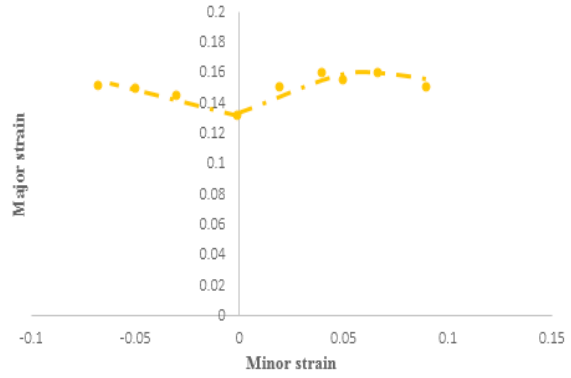

Fig. 11. Forming limit diagram after 1.5hr

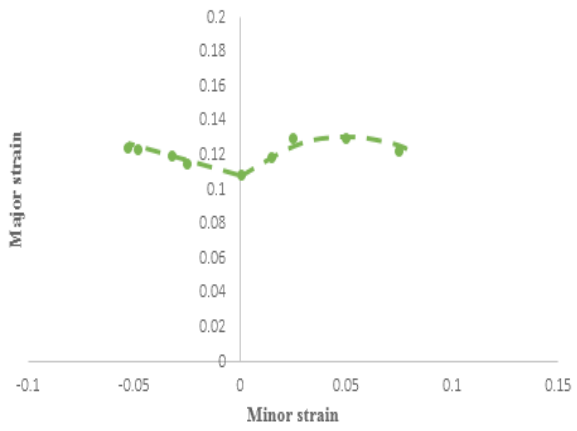

Fig. 12. Forming limit diagram after 4hr

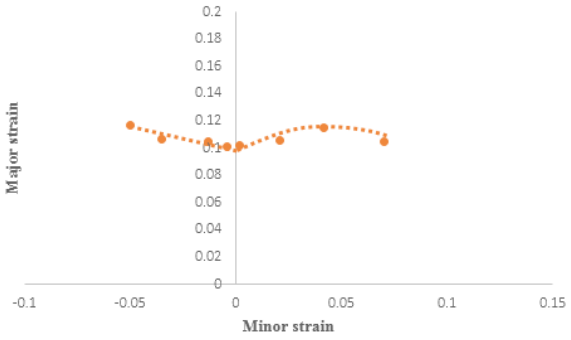

Fig. 13. Forming limit diagram after 24hr

Finally, in Fig. 14 it can be compared the FLD in all conditions at a glance.

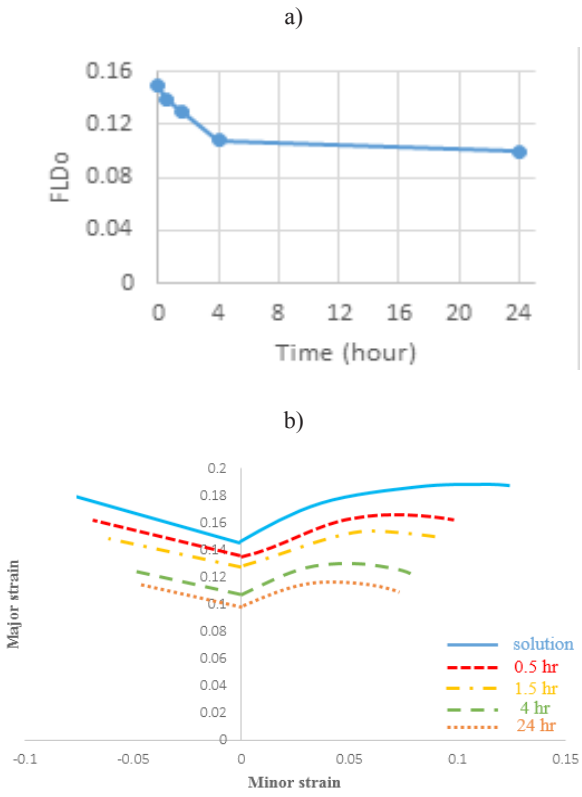

Fig. 14. a) FLD_o variations according to time-consuming b) Forming limit diagram for all heat treatment conditions

Table 2. The forming and the mechanical properties of Al 2024 alloy

Sample	Micro-hardness (HV)	Ultimate Tensile Strength, (Mpa)	Yield Strength, (Mpa)	FLD_o	Elongation at Break, %
Solution	70	313	110	0.149	15.4
Ageing at 0.5hr	97	329	130	0.139	14.8
Ageing at 1.5hr	110	343	160	0.13	14.2
Ageing at 4hr	136	385	205	0.108	13.3
Ageing at 24hr	145	411	247	0.1	12.9

With the comparison between the FLCs in Fig. 14, bypassing of time, the curves convexity increased that the cause is increasing the intensity of brittle fracture in specimens.

3.4. Microstructural Investigations

For observing the variations in specimens, first, we polished the surface of the sample by using emery papers of different grades followed by their polishing using 3μm Al_2O_3 particles. The micro-structural pictures were investigated for four ageing times. In Fig. 15, the pictures with magnification 1000X are displayed. As for being seen in this figure by passing of ageing time the precipitates were changed, and the number and size of them were increased, so that this increasing up to 4hr had most of its growth, and from 4 to 24hr this increasing was fewer, and just the precipitates distribution increased. It is noteworthy that the ideal distribution could be achieved when the precipitations have a medium size because when the particles have a big size, their number for prevention against dislocations are not enough and when they are very small, they can't stop the dislocations as well [26, 27].

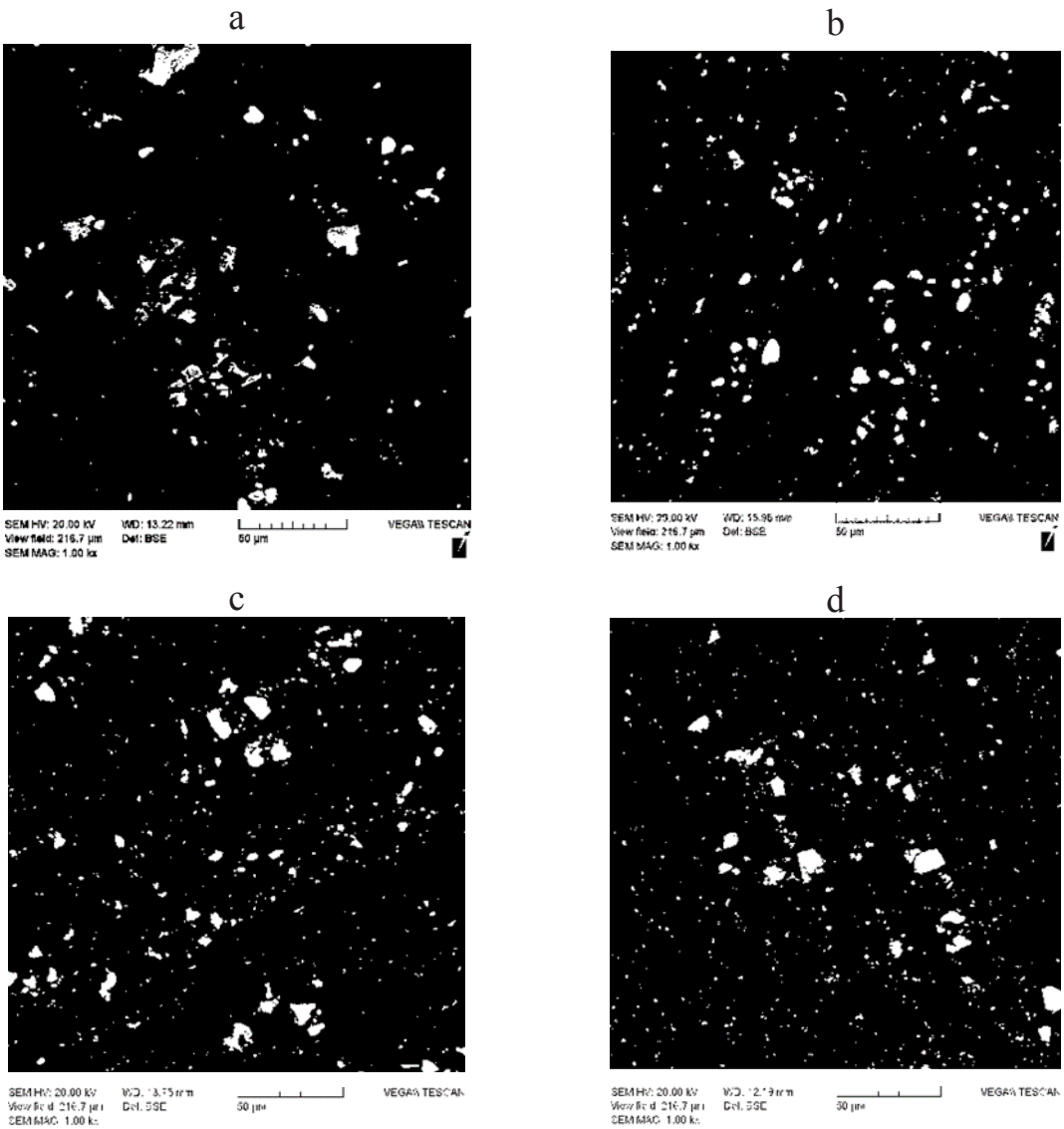

Fig. 15. SEM pictures at times a) 0.5h b) 1.5h c) 4h d) 24h with a magnification of 1000X

It is necessary to mention that for more clarity of photographs and better determinations of precipitates and particles, the figures were changed to more color contrast by software [28-34].

In Fig. 16 it can be seen the SEM pictures by greater magnifications. In this figures, community and growing the precipitates are illustrated.

By observing Fig. 15 and Fig. 16 it can be seen that by ageing the specimens up to 24h, a lot of white and dark gray precipitates and particles produced, that each of them represent a specific phase with different chemical composition in (Fig. 17). Also at some different place of the matrix, clustering of the particles or precipitations can be seen.

In 2024-T4 alloys often the precipitates Al_2CuMg in a sphere shape, (Mn, Fe) $SiAl_{12}$ with Irregular shape, Al_7Cu_2Fe with Dispersed particles $Cu_2Mn_3Al_{20}$, are formed. Kind of precipitates Al_2CuMg which formed in the ageing process that is many fines which seen just by TEM. These precipitates called S particle. The study's conclusions show that there are two kinds of an

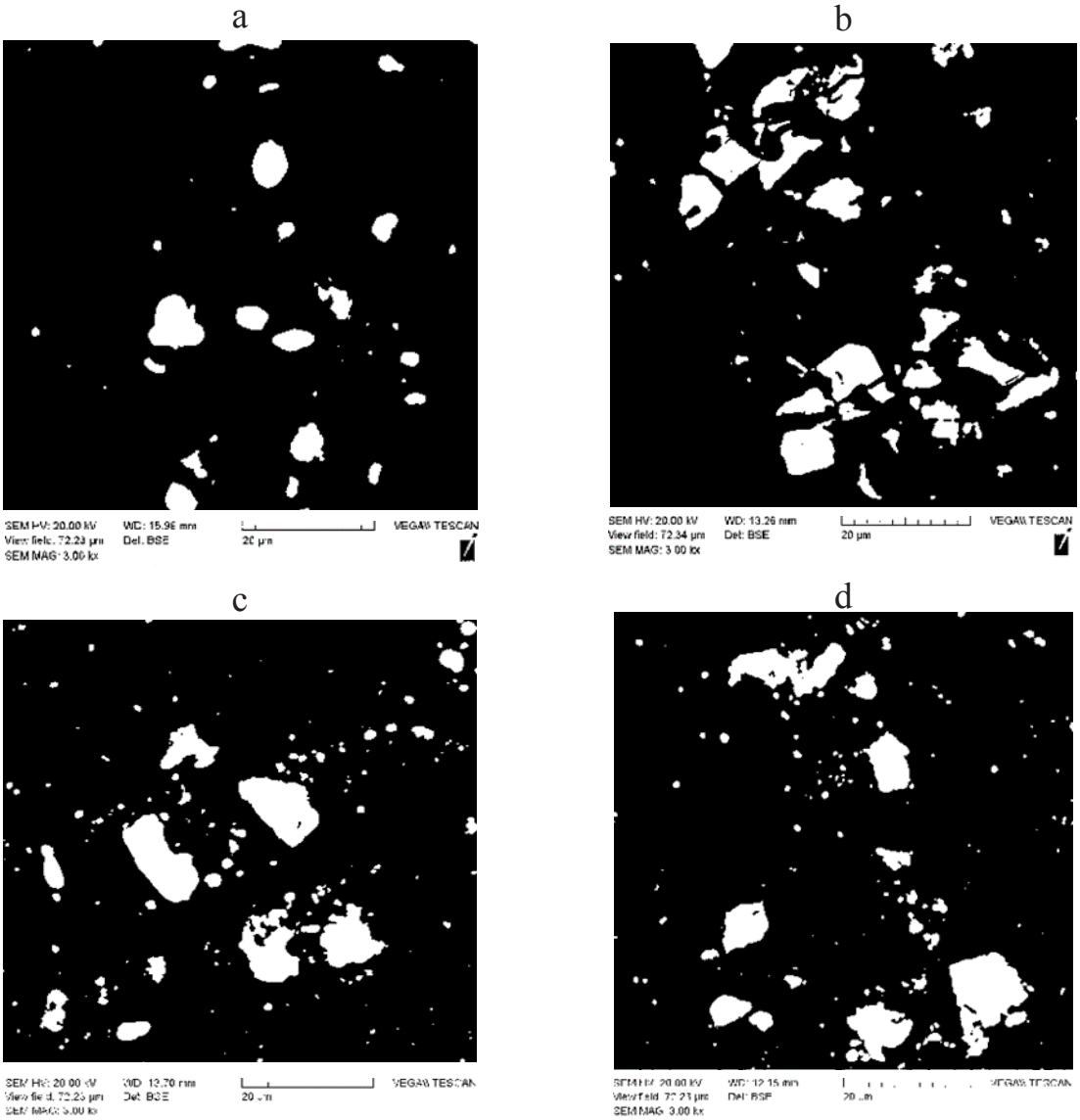

Fig. 16. SEM pictures at times a) 0.5h b) 1.5h c) 4h d) 24h with a magnification of 3000X

intermetallic particle in aluminum alloys Al-Cu-Mg. First one the particles involve Fe and Mn, the second one the particles involved Cu and Mg. By The presence of particles Fe and Mn in these alloys, the Equilibrium phases Al_6(Cu, Fe) and Al6Mn are formed. But in Non-equilibrium conditions, there is the possibility of making particles Al_6(Cu, Fe, Mn). Because often aluminum production condition, such as 2024 alloys, are Non-equilibrium, the presence of mentioned particles were reported. Particles involved Fe and Mn in aluminum alloys are formed during the freezing process and are insoluble in aluminum background phase [28, 29].

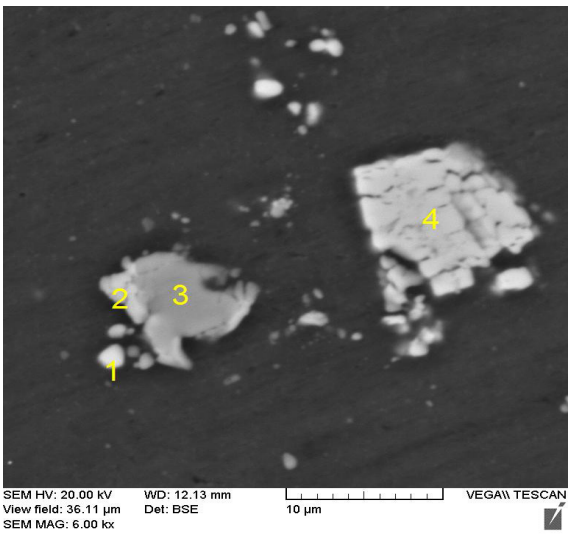

	Elt	W%	A%
1	Mg	1.18	1.49
	Al	75.70	86.61
	Si	0.44	0.48
	Mn	0.58	0.33
	Fe	5.26	2.91
	Cu	16.84	8.18
	Total	100	100
2	Mg	1.58	1.97
	Al	78.54	88.04
	Si	0.31	0.34
	Mn	0.85	0.47
	Fe	4.18	2.26
	Cu	14.55	6.92
	Total	100	100
3	Mg	0.46	0.59
	Al	69.48	79.80
	Si	5.89	6.50
	Mn	6.26	3.53
	Fe	12.54	6.96
	Cu	5.36	2.62
	Total	100	100
4	Mg	0.14	0.20
	Al	58.92	75.87
	Si	0.64	0.79
	Mn	2.83	1.79
	Fe	11.40	7.09
	Cu	26.06	14.25
	Total	100	100

Fig. 17. EDS results for different phases of precipitates at ageing for 24h by magnification 6000X

4. Conclusions

This paper investigated how natural ageing heat treatment influences the mechanical properties, microstructural variations and forming limit diagrams of Al-Cu-Mg alloy sheets. The achieved results are as follows:

1. It is evident that in this alloy by ageing up to 4h, the hardness was increased to 94% in comparison to solution treatment and from 4h to 24h the variation was with a mild slope, and the hardness growth was just 6.6% in comparison with ageing for 4h.
2. It could be illustrated that by increasing the ageing time, the yield and the ultimate strength increased, whereas the elongation to failure decreased. By ageing from solution treatment up to 24 hours, the ultimate tensile strength increased from 313MPa to 411MPa that show 31% growth and the elongation at break decreased from 15.4% to 12.9%, which show 19% reduction.
3. According to forming limit diagrams by comparison between FLDo points from solution condition to ageing for 24h, it was observed by passing the time, the forming limits were decreased and from 1.5h to 4hr it was occurred a noticeable decrease that the cause was more precipitation distribution and then a full brittle fracture which was occurred in this condition.
4. By investigating the microstructure figures observed that bypassing of ageing time the precipitates were changed and the number and size of them were increased, so that this increasing up to 4hr had most of its growth, and from 4hr to 24h this increasing was fewer, and just the precipitates distribution increased.

REFERENCES

1. Rahmatabadi, D., Hashemi, R., "Experimental evaluation of forming limit diagram and mechanical properties of nano/ultra-fine grained aluminum strips fabricated by accumulative roll bonding", Int. J. Mater. Res., 2017, 108, 1036-1044.
2. Mirfalah-Nasiri, S.M., Basti, A., Hashemi, R., "Forming limit curves analysis of aluminum alloy considering the through-thickness normal stress, anisotropic yield functions and strain

rate, Int. J. Mech. Sci., 2016, 117, 93-101.
3. Mamusi, H., Masoumi, A., Hashemi, R., Mahdavinejad, R., "A novel approach to the determination of forming limit diagrams for tailor-welded blanks." J. Mater. Eng. Perform., 2013, 22, 3210-3221.
4. Habibi, M., Hashemi, R., Sadeghi, E., Fazaeli, A., Ghazanfari, A., Lashini, H., "Enhancing the Mechanical Properties and Formability of Low Carbon Steel with Dual-Phase Microstructures", J. Mater. Eng. Perform., 2016, 25, 382–389.
5. Standard test method for determining forming limit curves, ASTM-E-2218-02.
6. ISO-12004-2, Metallic materials-sheet and strip-determination of forming-limit curves — part 2: determination of forming limit curves in the laboratory, 2008, 2, 1-6.
7. Bagaryatsky, Y. A., "Structural changes on ageing Al–Cu–Mg alloys." Doklady Akademii Nauk,1952, SSSR 87.1: 397-562.
8. Perlitz, H., Westgren, A., "The crystal structure of AlCuMg, Ark. Kemi. Mineral. Geol.,1943, 16B, 1–5.
9. Mondolfo, L. F., "Aluminum Alloys: Structure and Properties", Butterworths, London, 1976.
10. Gupta, A. K., Gaunt, P., Chaturvedi, M. C., "The crystallography and morphology of the S –phase precipitate in an Al (CuMg) alloy", Phil. Mag. A, 1987, 55, 375–387.
11. Ringer, S. P., Hono, K., Polmear, I. J. and Sakurai, T., "Precipitation processes during the early stages of ageing in Al–Cu–Mg alloys", Appl." Surf. Sci., 1996, 94/95, 253–260.
12. Kilaas, R., Radmilovic, V., "Structure determination and structure refinement of Al2CuMg precipitates by quantitative high-resolution electron microscopy", Ultramicroscopy, 2001, 88, 63–72.
13. Genevois, C., Deschamps, A., Denquin, A., Doisneau-cottignies, B., "Quantitative investigation of precipitation and mechanical behaviour for AA2024 friction stir welds", Acta Mater., 2005, 53, 2447–2458.
14. Abis, S., Massazza, M., Mengucci, P., Riontino, G., "Early ageing mechanisms in a high-copper AlCuMg alloy, Scr". Mater., 2001, 45, 685– 691.
15. Feng, Z., Yang, Y., Huang, B., "Precipitation process along dislocations in Al–Cu–Mg alloy during artificial ageing", Mater. Sci. Eng. A, 2010, 528, 706–714.
16. Wang, S. C., Starink, M. J., Gao, N., "Precipitation hardening in Al–Cu– Mg alloys", Scr. Mater., 2006, 54, 287-291 .
17. Gurugubelli, S. N., "The effect of ageing on impact toughness and microstructure of 2024 Al–Cu–Mg alloy", World Acad. Sci., Eng. Technol., 2010, 62, 648–650.
18. Dilmec, M., Halkaci, H., Ozturk, F., Livatyali, H., Yigit, O., "Effects of sheet thickness and anisotropy on forming limit curves of AA2024-T4". Int. J. Adv. Manuf. Technol., 2013, 67, 2689-2700 .
19. Moy, K. S., Weiss, M., Xia, J., Sha, G., Ringer, P., Ranzi, G., "Influence of heat treatment on the microstructure, texture and formability of 2024 aluminium alloy". Mater. Sci. Eng. A., 2012, 552, 48-60 .
20. Afzal, N., Shah, T., Ahmad, R., "Microstructural Features and Mechanical Properties of Artificially Aged AA2024". Strength of Materials, 2013, 45, 684-692.
21. Dilmeç, M., Arıkan, H., "Effect of Solution Heat Treatment Conditions on the Mechanical Properties and Formability for AA 2024 Alloy". In Applied Mechanics and Materials, 2014, 686, 3-9.
22. Handbook, A. S. M. Volume 4: Heat Treating. ASM International, 1991, 4, 1-926.
23. Hajian M., Assempour, A., "Experimental and numerical determination of forming limit diagram for 1010 steel sheet: a crystal plasticity approach", Int. J. Adv. Manuf. Technol., 2014, 76, 1757–1767.
24. Rahimi, H., M. Sedighi, M. and Hashemi, R., "Forming limit diagrams of fine-grained Al 5083 produced by equal channel angular rolling process", Proc. Inst. Mech. Eng. Part L J. Mater. Des. Appl., 2016, 1–9 . Doi: 10.1177/1464420716655560.
25. Ozturk, F., Sisman, A., Toros, S., Kilic, S., Picu, R. C., "Influence of ageing treatment on mechanical properties of 6061 aluminum alloy", Mater. Des., 2010, 31, 972–975.
26. Ernst, F., "Precipitation Hardening of Al–Si–Mg Alloys. EMSE-290 Materials Laboratory III, Spring semester", case Western Reserve University, Cleveland, OH, 2004.
27. Ozturk, F., Esener, E., Toros, S., Picu, C. R.,

Effects of ageing parameters on formability of 6061-O alloy, Mater. Des., 2010, 31, 4847–4852.
28. Barcellona, A., Buffa, G., Fratini, L., Palmeri, D., On microstructural phenomena occurring in friction stir welding of aluminium alloys. J. Mater. Proc. Technol., 2006, 177, 340-343.
29. Charit, I., Mishra, R.S., High strain rate superplasticity in a commercial 2024 Al alloy via friction stir processing. Mater. Sci. Eng. A., 2003, 359, 290-296.
30. Shabani, A., Toroghinejad, M. R., Shafyei, A., Investigating the formation of intermetallic compounds and the variation of bond strength between Al-Cu layers after annealing in presence of nickel between layers, Iran. J. Mater. Sci. Eng., 2016, 13, 35-43.
31. Mirzakouchakshirazi, H., Eivani, A.R., Kheirandish, Sh., Effect of post-deformation annealing treatment on interface properties and shear bond strength of Al-Cu bimetallic rods produced by equal channel angular pressing, Iran. J. Mater. Sci. Eng., 2017, 14, 25-34.
32. Torabzadeh Kashi, H., Bahrami, M., Shahbazi Karami , J., Faraji, Gh., Microstructure and mechanical properties of the ultrafine-grained copper tube produced by severe plastic deformation, Iran. J. Mater. Sci. Eng., 2017, 14, 32-40.
33. Rahmatabadi, D., Hashemi, R., Mohammadi, B., Shojaee, T., Experimental evaluation of the plane stress fracture toughness for ultra-fine grained aluminum specimens prepared by accumulative roll bonding process, Mater. Sci. Eng. A., 2017, 708, 301-310.
34. Borji, S., Zangeneh-madar, K., Ahangarkani, M., Valefi, Z., The feasibility of W-Cu composite production by submicron particles addition and infiltration, Iran. J. Mater. Sci. Eng., 2017, 14, 1-11.